Modeling Sample Disorder in Site-Specific Dichroism Studies of Uniaxial Systems

Itamar Kass, Eyal Arbely, and Isaiah T. Arkin
The Alexander Silberman Institute of Life Sciences, Department of Biological Chemistry, The Hebrew University, Jerusalem, Israel

ABSTRACT Site-specific infrared dichroism is an emerging method capable of proposing a model for the backbone structure of a transmembrane α-helix within a helical bundle. Dichroism measurements of single, isotopically enhanced vibrational modes (e.g., Amide I $^{13}C{=}^{18}O$ or Gly CD_2 stretching modes) can yield precise orientational restraints for the monomer helix protomer that can be used as refinement constraints in model building of the entire helical bundle. Essential, however, for the interpretation of the dichroism measurements, is an accurate modeling of the sample disorder. In this study we derive an enhanced and more realistic modeling of the sample disorder based on a Gaussian distribution of the chromophore around a particular angle. The enhanced utility of the Gaussian model is exemplified by the comparative data analysis based on the aforementioned model to previously employed models.

INTRODUCTION

Membrane proteins are involved in a large number of biological functions, such as respiration, signal transduction, and molecular transport. Using statistical analysis of various genomes, it was shown that the proportion of membrane proteins is between 20% and 35% of all encoded proteins (Wallin and von Heijne, 1998; Stevens and Arkin, 2000). Moreover, many genetic disorders are directly related to membrane proteins and it is estimated that >70% of all currently available drugs act on membrane proteins. Our understanding of these processes, and as a result the success of rational drug design, depends upon knowledge of the structure of membrane proteins. However, in contrast to water-soluble proteins, the structure of membrane proteins is not as easily solved using standard methods such as solution nuclear magnetic resonance (NMR) spectroscopy or x-ray diffraction.

This paucity of structural information on membrane protein has stemmed the development of alternative approaches yielding orientational restraints, capable of deriving structures of membrane proteins. One such method, which yields detailed backbone structures of membrane systems, is solid-state NMR (Opella et al., 2002; Arora and Tamm, 2001; de Groot, 2000). Using this method the structure of the protomer backbone, and a detailed description of its orientation with respect to the bilayer, can be derived by using orientational restraints (Bertram et al., 2000). Examples include: the M2 protein from Influenza A (Kovacs et al., 2000; Wang et al., 2001), gramicidin A (Ketchem et al., 1993), the M2 channel-lining segment from nicotinic acetylcholine receptor (Opella et al., 1999), and the major pVIII coat protein of *fd* filamentous bacteriophage (Marassi and Opella, 2003).

Submitted November 26, 2002, and accepted for publication September 17, 2003.

Address reprint requests to Isaiah T. Arkin, Tel./Fax: 972-2-658-4329; E-mail: arkin@cc.huji.ac.il.

© 2004 by the Biophysical Society

0006-3495/04/04/2502/06 $2.00

Recently, site-specific infrared dichroism studies (SSID) were able to derive similar orientational restraints, yielding structural models of membrane α-helical bundles (Kukol et al., 1999, 2002; Kukol and Arkin, 1999, 2000; Torres et al., 2000, 2002). Thus, the promise that SSID has shown as an additional method capable of yielding precise structural models of membrane proteins motivates efforts to increase its accuracy. It is for this reason that, in the present study, the analysis of sample disorder (critical to the success of SSID) is expanded in terms of a more realistic and rigorous mathematical representation.

THEORY

Dipole moment orientation

The orientation of a transition dipole moment of a single vibrational mode $\vec{\mathbf{P}}$ in an α-helix can be expressed as a function of several geometrical parameters: 1), the helix tilt angle β; 2), the angle α relating the helix axis and the dipole moment (in the case of the amide I mode it is measured to be 141°; Tsuboi, 1962); and 3), the rotational pitch angle ω around the helix axis (see Fig. 1). The orientation of a canonical helix with respect to the axes can therefore be readily extracted given a perfect dichroic ratio from a site-directed Fourier transform infrared (FTIR) dichroism measurement. However, in practice the sample may actually be less than perfectly ordered; although a fraction of the helices will be tilted from the membrane normal by the angle β, others may not. Clearly the accuracy of the derived helical tilt and pitch angles depends on the accuracy of the proposed model.

The absorption by vibrational modes located within disordered helices will change the observed dichroism and affect the calculated helix tilt and pitch angles. Thus, estimates of the helix tilt and pitch angles will then depend on the order of the sample. Following Fraser (1953), previous analyses of infrared spectroscopy dichroism results were discussed in terms of a model in which a certain fraction f, of the helices, was thought to be perfectly tilted with respect to the membrane normal by the angle β, and the remaining fraction $(1 - f)$, perfectly random (Arkin et al., 1997). Clearly the accuracy of the derived helical tilt and pitch angles depends on the accuracy of the proposed model.

To increase the accuracy of the derived helix tilt and pitch angles, a new physical model was derived and implemented in which a Gaussian distribution function was used. In this study, we use the new model to evaluate, using previous experimentally published results, the helices' director mean tilt angle μ and the sample disorder σ, correlated to β and f in the previous model, respectively.

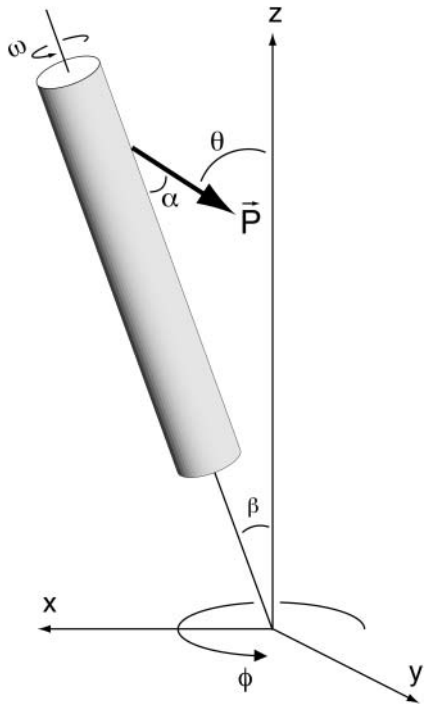

FIGURE 1 Schematic representation of the geometric parameters that are used to define a chromophore's transition dipole moment orientation. The helix director is tilted from the z axis by the angle β, containing a vibrating bond $\vec{\mathbf{P}}$ related to the helix director by the angle α. The bond is positioned with a rotational pitch angle ω around the helix director. The angle θ is the absolute angle between the transition dipole moment and the z axis. Uniaxial symmetry results in rotational averaging around the z axis by the angle ϕ.

Dichroic ratio

The experimentally measured dichroic ratio, $\mathcal{R}$, is defined as the absorption ratio between parallel and perpendicular polarized light of a chromophore whose transition dipole vector is $\vec{\mathbf{P}}$ (see Fig. 1),

$$\mathcal{R} \equiv \frac{\mathcal{A}_{\parallel}}{\mathcal{A}_{\perp}}. \tag{1}$$

Integrated absorption coefficients

The absorption of light is equal to the squared scalar product between the axial electric field components $\mathcal{E}_x$, $\mathcal{E}_y$, and $\mathcal{E}_z$ and the corresponding dimensionless integrated absorption coefficients $\mathcal{K}_x$, $\mathcal{K}_y$, and $\mathcal{K}_z$ (Arkin et al., 1997). In the geometrical configuration of attenuated total internal reflection (Harrick, 1967) the dichroic ratio is given by

$$\mathcal{R} = \frac{\mathcal{E}_z^2\mathcal{K}_z + \mathcal{E}_x^2\mathcal{K}_x}{\mathcal{E}_y^2\mathcal{K}_y}. \tag{2}$$

The integrated absorption coefficients $\mathcal{K}_x(\omega)$, $\mathcal{K}_y(\omega)$, and $\mathcal{K}_z(\omega)$, for a single chromophore $\vec{\mathbf{P}}$, are related to the square of the projection of $\vec{\mathbf{P}}$ over the axes x, y, and z, respectively (see Arkin et al., 1997, for derivation), as

$$\begin{aligned}\mathcal{K}_x(\omega) = &\frac{\cos(\beta)^2\cos(\omega)^2\sin(\alpha)^2}{2} \\ &+ \cos(\alpha)\cos(\beta)\cos(\omega)\sin(\alpha)\sin(\beta) \\ &+ \frac{\cos(\alpha)^2\sin(\beta)^2}{2} + \frac{\sin(\alpha)^2\sin(\omega)^2}{2},\end{aligned} \tag{3}$$

$$\mathcal{K}_y(\omega) = \mathcal{K}_x(\omega), \tag{4}$$

$$\begin{aligned}\mathcal{K}_z(\omega) = &\cos(\alpha)^2\cos(\beta)^2 \\ &- 2\cos(\alpha)\cos(\beta)\cos(\omega)\sin(\alpha)\sin(\beta) \\ &+ \cos(\omega)^2\sin(\alpha)^2\sin(\beta)^2.\end{aligned} \tag{5}$$

Integration over all possible pitch angles yields $\mathcal{K}_x(\langle\omega\rangle)$, $\mathcal{K}_y(\langle\omega\rangle)$, and $\mathcal{K}_z(\langle\omega\rangle)$, which are used to calculate the dichroic ratio for an α-helix with vibrational modes rotationally distributed in a random fashion (Arkin et al., 1997), as

$$\begin{aligned}\mathcal{K}_x(\langle\omega\rangle) = &\frac{\sin(\alpha)^2}{4} + \frac{\cos(\beta)^2\sin(\alpha)^2}{4} \\ &+ \frac{\cos(\alpha)^2\sin(\beta)^2}{2},\end{aligned} \tag{6}$$

$$\mathcal{K}_y(\langle\omega\rangle) = \mathcal{K}_x(\langle\omega\rangle), \tag{7}$$

$$\mathcal{K}_z(\langle\omega\rangle) = \cos(\alpha)^2\cos(\beta)^2 + \frac{\sin(\alpha)^2\sin(\beta)^2}{2}. \tag{8}$$

Sample disorder

In Eq. 2, sample disorder is not taken into account, in that all helices are assumed to share the same tilt angle (i.e., there is no variation in β).

Fractional sample order

In the previous model, following Fraser (1953), the fraction of perfectly ordered material around a particular helix tilt is denoted f, and thus $1 - f$ consists of the random fraction. An appropriate and mathematically simple correction for the integrated absorption coefficients yields the desired function describing the dichroic ratio, as

$$\mathcal{R} = \frac{\mathcal{E}_z^2\left(f\mathcal{K}_z + \frac{1-f}{3}\right) + \mathcal{E}_x^2\left(f\mathcal{K}_x + \frac{1-f}{3}\right)}{\mathcal{E}_y^2\left(f\mathcal{K}_y + \frac{1-f}{3}\right)}. \tag{9}$$

Gaussian distribution of sample order

The utility of the fractional distribution function clearly rests in its mathematical simplicity. However, it is equally clear that in reality the order in which helices tilt from the lipid bilayer may be better approximated by the mathematically more realistic Gaussian distribution, $F(\beta)$ (see below). Thus, the dichroic ratio of a single chromophore $\vec{\mathbf{P}}$, can be written as

$$\mathcal{R}_S = \frac{\mathcal{E}_z^2 \int_{-\infty}^{\infty} F(\beta)\mathcal{K}(\omega)_z d\beta + \mathcal{E}_x^2 \int_{-\infty}^{\infty} F(\beta)\mathcal{K}(\omega)_x d\beta}{\mathcal{E}_y^2 \int_{-\infty}^{\infty} F(\beta)\mathcal{K}(\omega)_y d\beta}, \quad (10)$$

whereas the dichroic ratio of an α-helix with vibrational modes rotationally distributed in a random fashion, can be written as

$$\mathcal{R}_H = \frac{\mathcal{E}_z^2 \int_{-\infty}^{\infty} F(\beta)\mathcal{K}(\langle\omega\rangle)_z d\beta + \mathcal{E}_x^2 \int_{-\infty}^{\infty} F(\beta)\mathcal{K}(\langle\omega\rangle)_x d\beta}{\mathcal{E}_y^2 \int_{-\infty}^{\infty} F(\beta)\mathcal{K}(\langle\omega\rangle)_y d\beta}. \quad (11)$$

According to the Gaussian distribution, the probability of finding a helix with a tilt angle β is given by

$$F(\beta) = \frac{1}{\sqrt{2\pi}\sigma} e^{\frac{-(\beta-\mu)^2}{2\sigma^2}}, \quad (12)$$

whereby μ and σ are the mean tilt angle and the standard deviation, respectively. Normalization maintains that integration of Eq. 12 from minus infinity to plus infinity equals 1.

Based on Eq. 12, it can be seen that the disorder of the sample is given by σ: Higher disorder of the sample will result in an increase in σ. The integrated absorption coefficients given in Eqs. 3–8 should therefore be multiplied by the normalization factor.

Integration of the normalized integrated absorption coefficients (see Appendix) from minus infinity to plus infinity, results in the averaged integrated absorption coefficient. See Appendix for derivations in which the geometrical relationship between the chromophore transition dipole moment and the helix axis is described by two angles, α and δ (Arkin et al., 1997). Thus we obtain the equations for the integrated absorption coefficients for a single chromophore on a helix, modeling the sample disorder as a Gaussian distribution,

$$\langle\mathcal{K}_x(\omega)\rangle = \int_{-\infty}^{\infty} \frac{1}{\sqrt{2\pi}\sigma} e^{\frac{-(\beta-\mu)^2}{2\sigma^2}} d\beta \mathcal{K}_x(\omega) = \frac{\cos(\alpha)^2\left(\frac{1}{2} - \frac{\cos(2\mu)}{2e^{2\sigma^2}}\right)}{2} + \frac{\left(\frac{1}{2} + \frac{\cos(2\mu)}{2e^{2\sigma^2}}\right)\cos(\omega)^2\sin(\alpha)^2}{2} + \frac{\cos(\alpha)\cos(\mu)\cos(\omega)\sin(\alpha)\sin(\mu)}{e^{\sigma^2}} + \frac{\sin(\alpha)^2\sin(\omega)^2}{2} \quad (13)$$

$$\langle\mathcal{K}_y(\omega)\rangle = \langle\mathcal{K}_x(\omega)\rangle, \quad (14)$$

$$\langle\mathcal{K}_z(\omega)\rangle = \int_{-\infty}^{\infty} \frac{1}{\sqrt{2\pi}\sigma} e^{\frac{-(\beta-\mu)^2}{2\sigma^2}} d\beta \mathcal{K}_z(\omega) = \cos(\alpha)^2\left(\frac{1}{2} + \frac{\cos(2\mu)}{2e^{2\sigma^2}}\right) + \left(\frac{1}{2} - \frac{\cos(2\mu)}{2e^{2\sigma^2}}\right)\cos(\omega)^2\sin(\alpha)^2 - \frac{2\cos(\alpha)\cos(\mu)\cos(\omega)\sin(\alpha)\sin(\mu)}{e^{\sigma^2}}. \quad (15)$$

By integrating the results of Eqs. 13–15 throughout all possible rotational pitch angles ω, we obtain the equations for the integrated absorption coefficients for an α-helix, modeling the sample disorder as a Gaussian distribution:

$$\langle\mathcal{K}_x(\langle\omega\rangle)\rangle = \int_{-\infty}^{\infty} \frac{1}{\sqrt{2\pi}\sigma} e^{\frac{-(\beta-\mu)^2}{2\sigma^2}} d\beta \mathcal{K}_x(\langle\omega\rangle) = \frac{\cos(\alpha)^2\left(\frac{1}{2} - \frac{\cos(2\mu)}{2e^{2\sigma^2}}\right)}{2} + \frac{\sin(\alpha)^2}{4} + \frac{\left(\frac{1}{2} + \frac{\cos(2\mu)}{2e^{2\sigma^2}}\right)\sin(\alpha)^2}{4}, \quad (16)$$

$$\langle\mathcal{K}_y(\langle\omega\rangle)\rangle = \langle\mathcal{K}_x(\langle\omega\rangle)\rangle, \quad (17)$$

$$\langle\mathcal{K}_z(\langle\omega\rangle)\rangle = \int_{-\infty}^{\infty} \frac{1}{\sqrt{2\pi}\sigma} e^{\frac{-(\beta-\mu)^2}{2\sigma^2}} d\beta \mathcal{K}_z(\langle\omega\rangle) = \cos(\alpha)^2\left(\frac{1}{2} + \frac{\cos(2\mu)}{2e^{2\sigma^2}}\right) + \frac{\left(\frac{1}{2} - \frac{\cos(2\mu)}{2e^{2\sigma^2}}\right)\sin(\alpha)^2}{2}. \quad (18)$$

RESULTS

Gaussian distribution results

Table 1 presents the results in which the Gaussian distribution model was used to solve site-specific dichroism data for all transmembrane α-helical bundles for which structures are available from other methods: human glycophorin A (GpATM) (Arkin et al., 1997), solution NMR structure in detergent micelles (MacKenzie et al., 1997), Influenza A M2 (Kukol et al., 1999), solid-state NMR (Wang et al., 2001; Wray et al., 1999), and HIV *vpu* (Kukol and Arkin, 1999) solid-state NMR (Marassi et al., 1999; Wray et al., 1999). When compared to the results obtained using NMR, significant similarity is observed to those obtained in this study. Differences between our results and that obtained by NMR results may arise from 1), different procedures which were used for the reconstitution of the TM peptides and 2), difference in experimental temperature.

TABLE 1 Comparison of literature values

	GpATM	M2	*vpu*
$\beta_{\text{independent data}}$	20°	33°	≤30° (Wray et al., 1999) 15 ± 5° (Marassi et al., 1999)
μ	24.77 ± 3.18°	30.3 ± 8.9°	5.6 ± 1.8°
$\omega_{\text{independent data}}$	341°	−57°	N/A
ω	314.11 ± 2.53°	−60.8 ± 7.2°	294.5 ± 7.1°
$\sigma_{\text{independent data}}$	N/A	N/A	N/A
σ	56.45 ± 9.69°	30.8 ± 9.3°	19.2 ± 4.8°

GpATM (MacKenzie et al., 1997), M2 (Kovacs and Cross, 1997), and *vpu* (Wray et al., 1999; Marassi et al., 1999) of the helix tilt angle β and the rotational pitch angle ω with results obtained from the Gaussian distribution model (data taken from M2, Kukol et al., 1999; and *vpu*, Kukol and Arkin, 1999) in which μ is used instead of β and σ is used as the order parameter. The literature rotational pitch angles are designated as $\omega_{\text{independent data}}$, whereas results from the Gaussian distribution model are designated as ω.

To analyze the SSID data, canonical helices were assumed (i.e., no gross distortion in the helix). Based on this assumption, the pitch angle, ω, between two adjacent amino acids is 100°. This assumption is examined by inspecting the helicity of the TM peptides using FTIR. In other words, the frequency of the observed amide mode belonging to the helix as well as the labeled site are indicative of the high degree of helicity of the peptides. Furthermore, in at least one instance the canonical nature of the transmembrane helix of the M2 protein from influenza has been shown by other methods (Wang et al., 2001).

The use of a Gaussian distribution model to solve SSID data for transmembrane systems is a fast experimental way to find the three main parameters which are used to describe the system: tilt angle, pitch angle, and the sample disorder. The tilt and pitch angles can be used as a basis for molecular dynamics search, which can yield a model for the system (Adams et al., 1995).

The results for the *vpu* TM domain are an example for the advantages of the SSID analysis using the Gaussian distribution model over other methods (such as NMR). For example, when comparing the single parameter obtained from NMR (Wray et al., 1999; Marassi et al., 1999), the Gaussian distribution model yields three parameters (tilt angle, pitch angle, and the measure of the sample disorder). Thus, the more realistic Gaussian model, albeit mathematically more complex (compare Eqs. 3–8 with Eqs. 13–18), is readily capable of yielding results which are in excellent agreement to those obtained previously using different methods.

Relationship between the fractional sample order *f* and σ

In previous implementations of site-specific dichroism, disorder was modeled by way of a fractional sample order, $0 \le f \le 1$ (Arkin et al., 1997). In the present study in which a Gaussian distribution is used, σ represents the disorder parameter. In Fig. 2 the relationship between f and σ are simulated, and as expected, both parameters are inversely correlated; the higher σ is, the lower f is, and vice versa. The values of f at Fig. 2 are restricted to $0 \le f \le 1$. The reason is that, inasmuch as σ is not normalized, it is possible to obtain simulated f values <0 or >1, bearing no physical meaning.

DISCUSSION

Any mathematical model of sample disorder used in the analysis of site-specific dichroism must stand by the following two criteria:

1. The model must accurately represent the disorder that takes place in the sample.
2. The model must not be too mathematically complex so as to prevent the finding of numerical solutions to the coupled equations which describe site-specific dichroism.

The Gaussian distribution model presented in this study is clearly a better description for sample disorder than the fractional sample order presented previously (Fraser, 1953). The main advantage of the Gaussian distribution model is embedded in the more realistic way in which it describes the physical system. According to the model proposed by Fraser (1953), the helix directors which are not related to the membrane normal (the z axis) by angle β (see Fig. 1) are perfectly random. (For example, the probability of finding a helix director at angle $\beta + 1°$ or at angle $\beta + 50°$ is equal.) As described later, this is not a correct description of the sample disorder of uniaxial systems. In such systems, the probability of finding a helix director tilted by angles distinct from β decreases as the angle difference (from the angle β) increases. Using a Gaussian distribution model, a better description of uniaxial systems sample disorder is at hand.

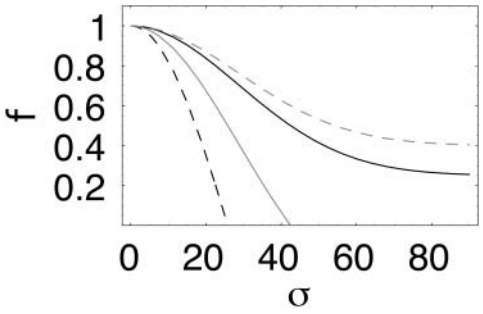

FIGURE 2 Calculated values for the order parameter f as function of the disorder parameter σ. Two-dimensional representation of the dependence f at σ for given β; in the graph, only values of $0 \le f \le 1$ are given. β-angles equal to 0°, 30°, 60°, and 90° are in black dashed and solid lines, and shaded dashed and solid lines, respectively.

As stated above, the measured dichroic ratio is a function of two parameters—the angle of the dipole moment, $\vec{P}$, and the disorder parameter. According to previous simulations of systems with varying β-angles and disorder parameter (Arkin et al., 1997), it was shown that for a system with a given β-angle, different disorder parameters will result in different dichroic ratios. Hence, proper description of the sample disorder is vital for proper calculation of β.

Major disorder in the sample may arise due to mosaicity variations in the membrane surface, which implies that the tilt angles of the helices are not random and equally distributed, but rather are located around a mean value (the angle μ). Mosaicity variations in the membrane surface arise mainly due to experimental difficulties in preparing a perfectly flat phospholipid bilayer. Minor disorder in the sample may also arise due to thermal fluctuations of membrane-embedded helices, inasmuch as those fluctuations are located around a mean value by their nature. The combination of these two factors gives a Gaussian distribution of the sample population around a mean value (the angle μ).

The obvious reason for the implementation of the fractional sample order model is its mathematical simplicity. However, modern computers are readily capable of numerically solving the coupled equations describing site-directed dichroism employing the Gaussian distribution model.

One final advantage of the Gaussian distribution model is the physical interpretability of the results which are yielded. Specifically, the width of the Gaussian distribution around a mean angle can be related to the membrane mosaicity which can be measured independently by other techniques such as x-ray reflectivity (Munster et al., 2002).

APPENDIX

The derivations of Eqs. 13–18 utilized the following integrals (Jeffrey, 1994):

$$\int_{-\infty}^{\infty} \frac{1}{\sqrt{2\pi}\sigma} e^{\frac{-(\beta-\mu)^2}{2\sigma^2}} d\beta = 1, \tag{A1}$$

$$\int_{-\infty}^{\infty} \frac{1}{\sqrt{2\pi}\sigma} e^{\frac{-(\beta-\mu)^2}{2\sigma^2}} \sin(\beta) d\beta = e^{-\sigma^2/2}\sin(\mu), \tag{A2}$$

$$\int_{-\infty}^{\infty} \frac{1}{\sqrt{2\pi}\sigma} e^{\frac{-(\beta-\mu)^2}{2\sigma^2}} \cos(\beta) d\beta = e^{-\sigma^2/2}\cos(\mu), \tag{A3}$$

$$\int_{-\infty}^{\infty} \frac{1}{\sqrt{2\pi}\sigma} e^{\frac{-(\beta-\mu)^2}{2\sigma^2}} \sin(\beta)^2 d\beta = \frac{1}{2} - \frac{1}{2}e^{-2\sigma^2}\cos(2\mu), \tag{A4}$$

$$\int_{-\infty}^{\infty} \frac{1}{\sqrt{2\pi}\sigma} e^{\frac{-(\beta-\mu)^2}{2\sigma^2}} \cos(\beta)^2 d\beta = \frac{1}{2} + \frac{1}{2}e^{-2\sigma^2}\cos(2\mu). \tag{A5}$$

Below are listed the derivations for the averaged integrated absorption coefficients when the geometrical relationship between the chromophore transition dipole moment and the helix axis is described by two angles: α and δ (Arkin et al., 1997). The integrated absorption coefficients before Gaussian normalization are given elsewhere (Arkin et al., 1997). Note that the following equations are equal to Eqs. 13–18 upon setting $\delta = 0$.

$$\begin{aligned}\langle \mathcal{K}_x(\omega)\rangle = {} & \frac{\cos(\alpha)^2\cos(\delta)^2\left(\frac{1}{2} - \frac{\cos(2\mu)}{2e^{2\sigma^2}}\right)}{2} + \frac{\cos(\delta)^2\left(\frac{1}{2} + \frac{\cos(2\mu)}{2e^{2\sigma^2}}\right)\cos(\omega)^2\sin(\alpha)^2}{2} + \frac{\cos(\omega)^2\sin(\delta)^2}{2} \\ & + \frac{\cos(\alpha)\cos(\delta)^2\cos(\mu)\cos(\omega)\sin(\alpha)\sin(\mu)}{e^{\sigma^2}} + \cos(\delta)\cos(\omega)\sin(\alpha)\sin(\delta)\sin(\omega) \\ & - \cos(\delta)\left(\frac{1}{2} + \frac{\cos(2\mu)}{2e^{2\sigma^2}}\right)\cos(\omega)\sin(\alpha)\sin(\delta)\sin(\omega) - \frac{\cos(\alpha)\cos(\delta)\cos(\mu)\sin(\delta)\sin(\mu)\sin(\omega)}{e^{\sigma^2}} \\ & + \frac{\cos(\delta)^2\sin(\alpha)^2\sin(\omega)^2}{2} + \frac{\left(\frac{1}{2} + \frac{\cos(2\mu)}{2e^{2\sigma^2}}\right)\sin(\delta)^2\sin(\omega)^2}{2},\end{aligned} \tag{A6}$$

$$\langle \mathcal{K}_y(\omega)\rangle = \langle \mathcal{K}_x(\omega)\rangle, \tag{A7}$$

$$\begin{aligned}\langle \mathcal{K}_z(\omega)\rangle = {} & \cos(\alpha)^2\cos(\delta)^2\left(\frac{1}{2} + \frac{\cos(2\mu)}{2e^{2\sigma^2}}\right) + \cos(\delta)^2\left(\frac{1}{2} - \frac{\cos(2\mu)}{2e^{2\sigma^2}}\right)\cos(\omega)^2\sin(\alpha)^2 \\ & - \frac{2\cos(\alpha)\cos(\delta)^2\cos(\mu)\cos(\omega)\sin(\alpha)\sin(\mu)}{e^{\sigma^2}} - 2\cos(\delta)\left(\frac{1}{2} - \frac{\cos(2\mu)}{2e^{2\sigma^2}}\right)\cos(\omega)\sin(\alpha)\sin(\delta)\sin(\omega) \\ & + \frac{2\cos(\alpha)\cos(\delta)\cos(\mu)\sin(\delta)\sin(\mu)\sin(\omega)}{e^{\sigma^2}} + \left(\frac{1}{2} - \frac{\cos(2\mu)}{2e^{2\sigma^2}}\right)\sin(\delta)^2\sin(\omega)^2.\end{aligned} \tag{A8}$$

The results for the helix dichroism are obtained by integrating the results of Eqs. 13–15 throughout all possible rotational pitch angles, ω:

$$\langle\mathcal{K}_x(\langle\omega\rangle)\rangle = \frac{\cos(\alpha)^2\cos(\delta)^2\left(\frac{1}{2}-\frac{\cos(2\mu)}{2e^{2\sigma^2}}\right)}{2} + \frac{\cos(\delta)^2\sin(\alpha)^2}{4} + \frac{\cos(\delta)^2\left(\frac{1}{2}+\frac{\cos(2\mu)}{2e^{2\sigma^2}}\right)\sin(\alpha)^2}{4} + \frac{\sin(\delta)^2}{4} + \frac{\left(\frac{1}{2}+\frac{\cos(2\mu)}{2e^{2\sigma^2}}\right)\sin(\delta)^2}{4}, \quad \text{(A9)}$$

$$\langle\mathcal{K}_y(\langle\omega\rangle)\rangle = \langle\mathcal{K}_x(\langle\omega\rangle)\rangle, \quad \text{(A10)}$$

$$\langle\mathcal{K}_z(\langle\omega\rangle)\rangle = \cos(\alpha)^2\cos(\delta)^2\left(\frac{1}{2}+\frac{\cos(2\mu)}{2e^{2\sigma^2}}\right) + \frac{\cos(\delta)^2\left(\frac{1}{2}-\frac{\cos(2\mu)}{2e^{2\sigma^2}}\right)\sin(\alpha)^2}{2} + \frac{\left(\frac{1}{2}-\frac{\cos(2\mu)}{2e^{2\sigma^2}}\right)\sin(\delta)^2}{2}. \quad \text{(A11)}$$

This research was supported in part by a grant from the Israel Science Foundation (784/01) to I.T.A.

REFERENCES

Adams, P. D., I. T. Arkin, D. M. Engelman, and A. T. Brunger. 1995. Computational searching and mutagenesis suggest a structure for the pentameric transmembrane domain of phospholamban. *Nat. Struct. Biol.* 2:154–162.

Arkin, I. T., K. R. MacKenzie, and A. T. Brunger. 1997. Site-directed dichroism as a method for obtaining rotational and orientational constraints for oriented polymers. *J. Am. Chem. Soc.* 119:8973–8980.

Arora, A., and L. K. Tamm. 2001. Biophysical approaches to membrane protein structure determination. *Curr. Opin. Struct. Biol.* 11:540–547.

Bertram, R., J. R. Quine, M. S. Chapman, and T. A. Cross. 2000. Atomic refinement using orientational restraints from solid-state NMR. *J. Magn. Reson.* 147:9–16.

de Groot, H. J. 2000. Solid-state NMR spectroscopy applied to membrane proteins. *Curr. Opin. Struct. Biol.* 10:593–600.

Fraser, R. D. B. 1953. The interpretation of infrared dichroism in fibrous protein structures. *J. Chem. Phys.* 70:1511–1515.

Harrick, N. 1967. Internal Reflection Spectroscopy, 1st Ed. Interscience Publishers, New York.

Jeffrey, A. editor.1994. Table of Integrals, Series, and Products, 5th Ed. Academic Press, London, UK.

Ketchem, R. R., W. Hu, and T. A. Cross. 1993. High-resolution conformation of gramicidin A in a lipid bilayer by solid-state NMR. *Science.* 261:1457–1460.

Kovacs, F. A., and T. A. Cross. 1997. Transmembrane four-helix bundle of influenza A M2 protein channel: structural implications from helix tilt and orientation. *Biophys. J.* 73:2511–2517.

Kovacs, F. A., J. K. Denny, Z. Song, J. R. Quine, and T. A. Cross. 2000. Helix tilt of the M2 transmembrane peptide from influenza A virus: an intrinsic property. *J. Mol. Biol.* 295:117–125.

Kukol, A., P. D. Adams, L. M. Rice, A. T. Brunger, and T. I. Arkin. 1999. Experimentally based orientational refinement of membrane protein models: a structure for the influenza A M2 H+ channel. *J. Mol. Biol.* 286:951–962.

Kukol, A., and I. T. Arkin. 1999. *Vpu* transmembrane peptide structure obtained by site-specific Fourier transform infrared dichroism and global molecular dynamics searching. *Biophys. J.* 77:1594–1601.

Kukol, A., and I. T. Arkin. 2000. Structure of the influenza C virus CM2 protein transmembrane domain obtained by site-specific infrared dichroism and global molecular dynamics searching. *J. Biol. Chem.* 275:4225–4229.

Kukol, A., J. Torres, and I. T. Arkin. 2002. A structure for the trimeric MHC class II-associated invariant chain transmembrane domain. *J. Mol. Biol.* 320:1109–1117.

MacKenzie, K. R., J. H. Prestegard, and D. M. Engelman. 1997. A transmembrane helix dimer: structure and implications. *Science.* 276: 131–133.

Marassi, F. M., C. Ma, H. Gratkowski, S. K. Straus, K. Strebel, M. Oblatt-Montal, M. Montal, and S. J. Opella. 1999. Correlation of the structural and functional domains in the membrane protein *Vpu* from HIV-1. *Proc. Natl. Acad. Sci. USA.* 96:14336–14341.

Marassi, F. M., and S. J. Opella. 2003. Simultaneous assignment and structure determination of a membrane protein from NMR orientational restraints. *Protein Sci.* 12:403–411.

Munster, C., A. Spaar, B. Bechinger, and T. Salditt. 2002. Magainin 2 in phospholipid bilayers: peptide orientation and lipid chain ordering studied by x-ray diffraction. *Biochim. Biophys. Acta.* 1562:37–44.

Opella, S. J., F. M. Marassi, J. J. Gesell, A. P. Valente, Y. Kim, M. Oblatt-Montal, and M. Montal. 1999. Structures of the M2 channel-lining segments from nicotinic acetylcholine and NMDA receptors by NMR spectroscopy. *Nat. Struct. Biol.* 6:374–379.

Opella, S. J., A. Nevzorov, M. F. Mesleb, and F. M. Marassi. 2002. Structure determination of membrane proteins by NMR spectroscopy. *Biochem. Cell Biol.* 80:597–604.

Stevens, T. J., and I. T. Arkin. 2000. Do more complex organisms have a greater proportion of membrane proteins in their genomes? *Proteins.* 39:417–420.

Torres, J., P. D. Adams, and I. T. Arkin. 2000. Use of a new label, $^{13}C{=}^{18}O$, in the determination of a structural model of phospholamban in a lipid bilayer. Spatial restraints resolve the ambiguity arising from interpretations of mutagenesis data. *J. Mol. Biol.* 300:677–685.

Torres, J., J. A. Briggs, and I. T. Arkin. 2002. Multiple site-specific infrared dichroism of CD3-ζ, a transmembrane helix bundle. *J. Mol. Biol.* 316: 365–374.

Tsuboi, M. 1962. Infrared dichroism and molecular conformation of a-form poly-*g*-benzyl-*L*-glutamate. *J. Polym. Sci.* 59:139–153.

Wallin, E., and G. von Heijne. 1998. Genome-wide analysis of integral membrane proteins from eubacterial, archaean, and eukaryotic organisms. *Protein Sci.* 7:1029–1038.

Wang, J., S. Kim, F. Kovacs, and T. A. Cross. 2001. Structure of the transmembrane region of the M2 protein H^+ channel. *Protein Sci.* 10: 2241–2250.

Wray, V., R. Kinder, T. Federau, P. Henklein, B. Bechinger, and U. Schubert. 1999. Solution structure and orientation of the transmembrane anchor domain of the HIV-1-encoded virus protein U by high-resolution and solid-state NMR spectroscopy. *Biochemistry.* 38:5272–5282.